

Effect of Electrolysis Parameters on the Specific Surface Area of Nickel Powder: Optimization using Box-Behnken Design

Ali H. Abbar

Chemical Engineering Department, University of Al-Qadisiyah, Iraq

E-mail: ali.abbar@qu.edu.iq, aliabbar68@yahoo.com

Received: 3 September 2018 / Accepted: 4 November 2018 / Published: 30 November 2018

The effect of three electrolysis operating parameters on the specific surface area of electrolytic nickel powder was investigated by adopting response surface methodology approach. Box-Behnken design was selected to optimize the electrodeposition process and to estimate the effects and interactions of current density, nickel sulfate concentration, and temperature. BETS, XRD-diffraction, optical microscopy, and atomic force microscopy (AFM) were used to characterize the nickel powder. The results revealed that the current density has the major effect on the specific surface area of nickel powder followed by nickel sulfate concentration. No significant effect of temperature was observed. The optimum conditions for producing nickel powder at a maximum specific surface area of $1.05\text{m}^2\text{g}^{-1}$ with an average particle size of 680.65 nm were a current density of 500mAcm^{-2} , nickel sulfate concentration of 20g L^{-1} , and an operating temperature of $38\text{ }^\circ\text{C}$. The corresponding current efficiency and energy consumption were 30%, 24.0 kWh kg^{-1} respectively. The prepared powder has better specifications than the industrial type (Type 255-carbonyl process). Analysis of variance (ANOVA) showed a high coefficient of determination (R^2) value of 0.978, thus ensuring an adequately adjustment of the second-order regression model with the experimental data. The conformity results proved that the Box-Behnken design could be efficiently used to optimize the process parameters for the electrolytic preparation of metal powders.

Keywords: electrodeposition, nickel powder, surface area, Box–Behnken design, optimization

1. INTRODUCTION

Nickel (Ni) powder has significant industrial applications. It is commonly used in the fabrication of electrodes for fuel cells, in the preparation of skeletons of the active material for alkaline batteries, anticorrosion paints, as catalysts in the chemical industries, and additionally several other applications that depend on the magnetic properties of nickel powder [1]. In powder metallurgy, mixtures of nickel and cobalt powders are used as constituents of metal-cutting and drilling hard metals. Nickel nanoparticles are used for targeted transfer of pharmaceutical and biologically active substances in

medicine and biology [2]. Suspensions of cobalt and nickel powders are used as oil additives for in-process repair of worn-out parts of automobile [3].

Ni powder can be made by different methods including the decomposition of nickel carbonyl, reduction of aqueous solution of a nickel salt with hydrogen under pressure (hydrometallurgical Sheritt process), water atomization of molten nickel, and electrochemical method [4]. Hydrometallurgical and atomization methods give relatively large particles and it is difficult to produce fine particle sizes economically while the other two methods give much finer particles [5].

The Electrochemical method provides Ni powders with particle size ranging from a few nanometers to several micrometers based on the operating conditions of the electrodeposition process. The main properties of the electrolytic Ni powder are dendritic shape of the particles, good compressibility, and the highest purity. By selecting the appropriate process parameters such as metal ion concentration, pH of the electrolyte, current density, cathode potential, temperature, type of the anode and cathode, and the distance between them, it is possible to control the crystallization mechanism to acquire the required shape and size of powder particles [6].

Ni powder electrodeposition was performed using two types of electrolyte: Acid electrolytes [7-9] and ammoniacal electrolytes [10-15]. The characteristic of acid electrolytes is that decreasing the nickel ion concentration in solution and increasing current density result in reducing the powder fragility. However, no oxides and basic salts existing in the structure of this powder and it could be stored in a dry place for an indefinite period without structure change or oxidation. For ammoniacal electrolytes, using of higher concentration of ammonia results in producing disperse and pure (without hydroxide impurities) nickel deposits [16]. A number of researchers [17-19] have recommended sulphate-chloride or all-chloride electrolytes for nickel powder electrodeposition. However, using such electrolytes is not always justified due to the unequal of the cathodic and anodic current efficiencies when nickel anodes are used, hence a necessary correction of nickel ion concentration is required for keeping a constant electrolyte composition during electrolysis. The use of all-sulphate electrolytes overcomes these shortcomings and gives superior results than sulphate-chloride electrolytes in spite of their lower electrical conductivity in comparison with sulphate-chloride or chloride electrolytes. [20].

Intensive studies have been conducted on the Nickel powder electrodeposition, most of these studies concerned with the investigation of the morphological structure (XRD, EDS, SEM) of Ni powders [8,14,16,21], while fewer studies were devoted to investigate the effect of operating variables on the particle size and apparent density of nickel powder [9,12,13,15,22]. However, no information is available on the effect of operating variables like current density, metal ion concentration, pH, and temperature on the specific surface area of Ni powder. Specific surface area as the most important physical property of Ni powder has an important effect on the physical and mechanical behavior of the powder metallurgy products prepared from this powder that have been used in different applications like electrical applications [23]. Therefore the investigation of the mutual effect of the operating variables on the specific surface area could be given a right picture of the strategy used for producing this powder at excellent properties.

Traditionally optimization of experimental conditions is usually achieved by altering a single variable while maintaining all other variables fixed at a certain set of conditions. This approach disregards the combined effects or interactions between variables. Another drawback is the increase in

the number of runs required to achieve the research which in turn cause an increase of time and expenses [24, 25]. To overcome this problem, response surface methodology (RSM) can be used as a motivating approach to recognize the process variables which drive to optimal response by conducting a less number of experiments. RSM is a combination of statistical and mathematical methods suitable for developing, improving, and optimizing processes parameters and can be utilized for estimating the relative significance of several operating parameters even in the existence of complex interactions [26]. Box–Behnken design is part of RSM, where each experimental factor is tested at three levels and the experimental response is compared with the predicted response [27, 28]. RSM has been successfully used in various sectors of the industry including metal removal processes [29], chemical and biological processes, drug and food industry [30]. To the best of our knowledge, the application of RSM in nickel powder electrodeposition is not yet reported.

The aim of this work is to study the effect of three operating variables including current density, nickel sulfate concentration, and temperature on the specific surface area of nickel powder and determine the optimal values of these variables using Box–Behnken design.

2. EXPERIMENTAL WORK

2.1. Materials

All chemicals used were of analytical grade (BDH) and the experimental solution was prepared using double distilled water. Electrodeposition of Nickel powder was conducted from a solution containing 1 M $(\text{NH}_4)_2\text{SO}_4$, 0.7 M NH_4OH with different concentrations of nickel sulfate ($\text{NiSO}_4 \cdot 7\text{H}_2\text{O}$).

2.2. Electrolytic cell

A Pyrex beaker (0.5 L) equipped with a polytetrafluoroethylene (PTFE) cover plate was used as a single compartment electrolytic cell for electrodeposition of nickel powder. A stainless steel (316-AISL) plate with dimensions (2 cm width \times 13 cm long) was used as cathode while a nickel plate (99.9%) having the same dimensions was used as anode. The active surface area of each electrode was 10 cm². The back face of the cathode was plated by an epoxy to inhibit of nickel electrodeposition. Moreover, the distance between the anode and the cathode was kept at 3 cm, and all runs were finished after a total charge of 20250 coulombs was passed. Power supply- model UNI-T: UTP3315TF-L was used to run the galvanostatic electrodeposition of nickel. To maintain the temperature constant during the electrolysis, the cell body was immersed in a water bath. Fig. 1 represents the schematic diagram of the electrochemical system. At the end of each run, nickel powder was easily removed from the cathode surface and washed with distilled water and neutralized with 0.1M HCl. After that, the powder was filtered and treated with an alcohol-acetone mixture (ethanol-acetone = 1:1) to remove water, then dried for 2 h in 120 °C. Finally the produced powder was weighed and kept in a small polyethylene plastic bottle.

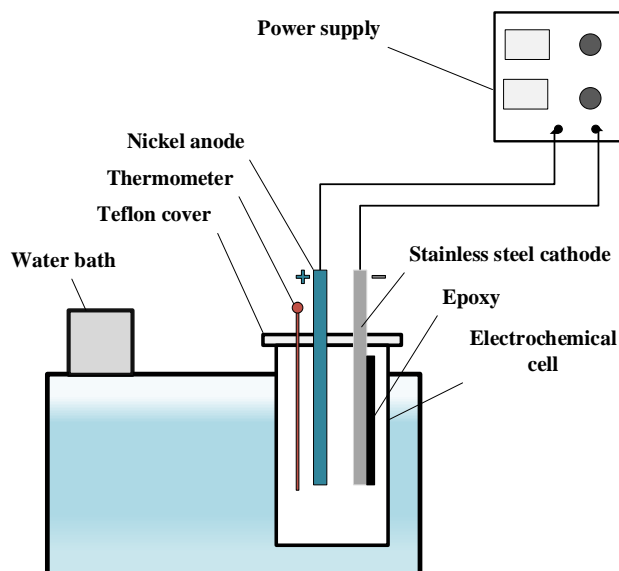


Figure 1. Electrochemical system

The current efficiency (CE) was calculated using Eqs. (1, 2) as follows [31, 39]:

$$m_{th} = \frac{M_w I t}{nF} \quad (1)$$

$$CE = \frac{m_{exp}}{m_{th}} \quad (2)$$

where m_{th} is the theoretical weight of nickel powder (g), m_{exp} is the actual weight of powder (g) produced in time (t), M_w is the atomic weight of Ni ($58.693 \text{ g mol}^{-1}$), I is the current in ampere, t is the time of electrodeposition in seconds, n is the valence of nickel (2), and F is Faraday constant (96486 C mol^{-1}).

The energy consumption was estimated using the following equation [32, 39]:

$$EC = \frac{2.778 \times 10^{-4} E I t}{m_{exp}} \quad (3)$$

Where EC is the energy consumption (kWh kg^{-1}) and E is the cell potential in volts

2.3. Characterization of Nickel powder

The specific surface area of nickel powder was measured by ASAP 2020 surface area analyzer using BET method. X-ray diffraction ($\text{CuK}\alpha$ radiation as the X-ray source, $\lambda = 1.54056 \text{ \AA}$) was used to identify the crystal structure of nickel powder. Atomic force microscopy (AFM) SPM-AA3000 (Angstrom Advanced Inc., USA) in contact mode was used to determine the average particle size of nickel powder. The AFM images were recorded over a scan area ($2 \mu\text{m} \times 2 \mu\text{m}$). The optical micrographs of nickel powder were obtained using Olympus BX51M with DP70 digital camera system.

2.4. Experimental design

Optimizing any process means establishing the optimum values of different parameters that gives a maximum desirable output. Different optimization methods have been used in the literatures; however,

RSM is the empirical preferred one. It is collective statistical and mathematical techniques depend on the fitting of a polynomial equation (empirical models) to the experimental data. This method creates a polynomial function which relates the response to the factors studied. To do that, it considers the factors only at certain levels (mostly -1, 0, 1). Response surface methodology produces an experimental design for model preparation, which is a particular set of runs defined by a matrix consisted of the different level combinations of the factors involved. RSM regressively fits the experimental results of the design to a model (first, second or higher order) then the coefficients involved in the model are determined. General designs relating to these models are: 1) First-Order Designs: The most well-known first-order designs are 2^k factorial (k is the number of control parameters) and Plackett–Burman designs. 2) Second-Order Designs: The most commonly employed second-order designs are the 3^k factorial, Box–Behnken, and the central composite designs [33].

Box–Behnken design (BBD) is an autonomous, rotatable quadratic design without inserted factorial or fractional factorial points where the combinations of variables are at the midpoints of the edges of the variable space and at the center. Besides, Box–Behnken design permits evaluating the response function at middle levels and permits the determination of the system performance at any experimental point within the range studied via suitable design and analysis of experiments [34]. In comparison with traditional factorial design methods, choosing Box–Behnken designs can decrease the number of experimental sets without reducing the optimization accuracy [35]. Therefore, Box–Behnken design offers more efficient matrices and is more economical design.

In Box–Behnken design, the number of runs was determined according to the formula $N=2k(k-1) + cp$, where k refers to the number of factors while (cp) represents the number of the central points. Besides, all factor levels should be regulated only at three levels (-1, 0, +1) with equally spaced intervals between these levels [33]. The quadratic equation model for predicting the optimal point based on this design can be expressed as follows [27]:

$$Y = \beta_0 + \sum \beta_i x_i + \sum \beta_{ii} x_i^2 + \sum \beta_{ij} x_i x_j + \varepsilon \quad (4)$$

Where Y is the predicted response, β_0 is the constant coefficient, β_i is the i th linear coefficient of the input factor x_i , β_{ii} is the i th quadratic coefficient of the input factor x_i , β_{ij} is the different interaction coefficients between the input factors x_i and x_j , and ε is the error of the model [27].

The optimization procedure consists of different consecutive steps; firstly the response of the statistically designed combinations is studied. Secondly, the coefficients of the model are determined by fitting the experimental data to the response functions. Thirdly, predicting the response of the fitted model, and finally the suitability of the model is checked by performing analysis of variance (ANOVA) [35].

In the present research, the Box–Behnken experimental design was used to investigate and confirm the electrolysis parameters affecting the specific surface area of electrochemically prepared nickel powder. Current density (A), nickel sulfate concentration (B), and temperature (C) were the input variables, while the specific surface area of nickel powder was chosen as a response (Y). Equation (4) then could be written as follows:

$$Y = \beta_0 + \beta_1 A + \beta_2 B + \beta_3 C + \beta_{12} AB + \beta_{13} AC + \beta_{23} BC + \beta_{11} A^2 + \beta_{22} B^2 + \beta_{33} C^2 \quad (5)$$

Based on the preliminary experimental results, the levels selected for the input variables are shown in Table 1. Table 2 displays the experimental design derived from BBD. Box–Behnken design

was generated by MINITAB-17 statistical analysis software. Statistical analysis of the model was achieved to evaluate the analysis of variance (ANOVA).

Table 1. Experimental design levels of the selected variables

Variables	Levels in Box–Behnken design		
Coded levels	Low(-1)	Middle(0)	High (+1)
Current density (mAcm^{-2})	100	300	500
$[\text{NiSO}_4 \cdot 7\text{H}_2\text{O}]$ (g L^{-1})	20	30	40
Temperature ($^{\circ}\text{C}$)	25	45	65

Table 2. Box–Behnken experimental design matrix

Run Order	Coded value			Real value.		
	A	B	C	Current density (mAcm^{-2})	$[\text{NiSO}_4 \cdot 7\text{H}_2\text{O}]$ (g L^{-1})	Temperature ($^{\circ}\text{C}$)
1	-1	-1	0	100	20	45
2	0	1	1	300	40	65
3	1	1	0	500	40	45
4	1	0	1	500	30	65
5	0	1	-1	300	40	25
6	-1	0	1	100	30	65
7	-1	1	0	100	40	45
8	-1	0	-1	100	30	25
9	1	-1	0	500	20	45
10	0	0	0	300	30	45
11	0	0	0	300	30	45
12	1	0	-1	500	30	25
13	0	-1	1	300	20	65
14	0	-1	-1	300	20	25
15	0	0	0	300	30	45

3. RESULTS AND DISCUSSION

3.1. Statistical analysis

In this research, the combined effects of current density, nickel sulfate concentration, and temperature at different levels on the specific surface area of nickel powder were investigated. Table 3 illustrates the data resulting from the experimental runs of the effect of these three variables on the

specific surface area. The values of current efficiency and power consumption for each experiment are mentioned also.

Table 3. Experimental results of Box–Behnken design with the predicted values

Run Order	A	B	C	m_{exp}^* (g)	E (Volt)	Surface area (m^2g^{-1})		CE (%)	EC (kWhkg^{-1})
						Actual	Predicted		
1	100	20	45	2.343	4.325	0.249	0.228	37.53	10.560
2	300	40	65	3.955	5.37	0.302	0.280	64.22	7.665
3	500	40	45	3.611	6.84	0.468	0.479	58.63	10.694
4	500	30	65	2.962	7.44	0.526	0.537	48.10	14.180
5	300	40	25	3.275	6.34	0.405	0.343	53.17	10.930
6	100	30	65	3.251	4.11	0.138	0.088	52.13	7.230
7	100	40	45	4.089	4.21	0.167	0.225	65.52	5.890
8	100	30	25	2.708	4.89	0.173	0.162	43.39	10.330
9	500	20	45	1.663	7.82	0.980	0.922	27.00	26.550
10	300	30	45	2.678	5.86	0.536	0.535	43.49	12.350
11	300	30	45	2.651	5.70	0.532	0.535	43.06	12.160
12	500	30	25	2.655	8.44	0.606	0.662	43.11	17.946
13	300	20	65	2.325	5.49	0.384	0.467	37.75	13.331
14	300	20	25	1.555	6.73	0.581	0.603	25.25	24.430
15	300	30	45	2.689	6.00	0.538	0.535	43.68	12.680

* $m_{\text{th}} = 6.159\text{g}$

The experimental results show that CE ranges between (25.52-65.52%). These results are in agreement with previous works [8, 11- 13] in spite of a higher current efficiency was observed in the present work. The lower CE results from the effect of side reaction (hydrogen evolution) which can't be avoided and the low value of Ni concentration. The hydrogen evolution increases as the concentration of metal ion decreases.

The experimental results were analyzed via Box–Behnken design to get an empirical model for the best response. The predicted results of this model are also reported in Table 2. The empirical model that describes the relationship between the response and input factors in coded terms can be expressed by the following quadratic equation:

$$Y = 0.5353 + 0.2371A - 0.1116B - 0.0497C - 0.0664A^2 - 0.0054B^2 - 0.1067C^2 - 0.1100AB - 0.0127AC + 0.0183BC \quad (6)$$

Equation (6) shows how the individual factors or double interactions affected the specific surface area. Negative coefficient values reveal that individual or double interaction factors inversely affect the specific surface area while positive coefficient values reveal that factors increase the specific surface area in the tested range. From the equation, it was observed that current density and the interaction of concentration with temperature have a positive effect on the specific surface area. Fig. 2 shows a plot of the experimental values of the specific surface area versus the predicted values using the model equation.

The coefficient of correlation (R^2) for fitting through origin is 0.9958 which confirms that the regression equation gives a precise description of the experimental data. It has successfully expressed the correlation between the three operating parameters and the specific surface area of nickel powder.

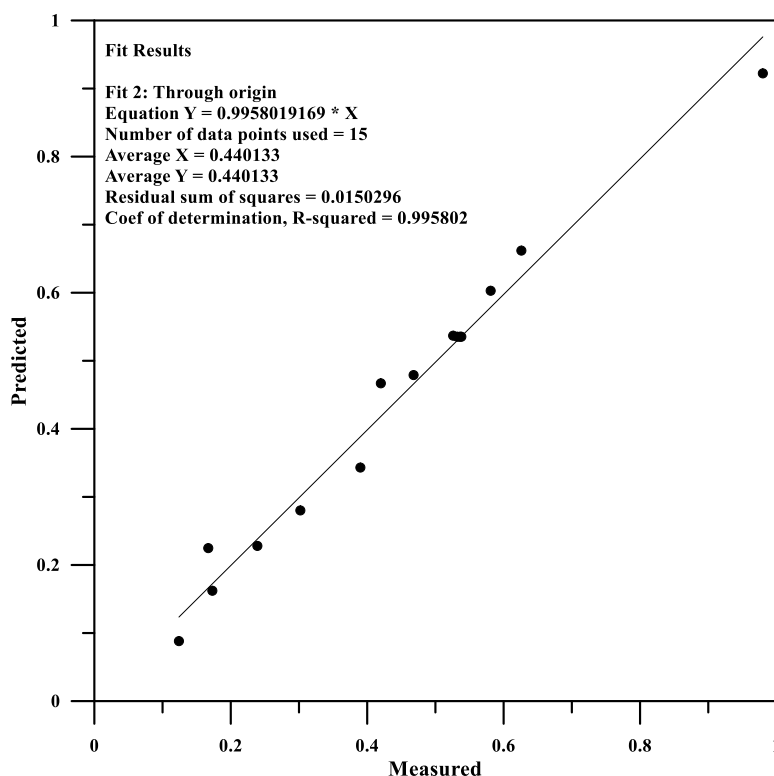


Figure 2. Relation between experimental and predicted surface area

Analysis of variance has been performed to determine the adequacy of the model representing the specific surface area; the results are given in Table 4. ANOVA as an analytical method is used to specify the significance of the model and its parameters where Fisher's F-test and Student's t-test (p-value) are used as criteria for this purpose. As a guideline, smaller p-values and larger F-values reveal more significant coefficient terms. ANOVA also splits the total variation in a set of data into individual parts accompanied with certain sources of variation to examine hypotheses on the model parameters [36].

Analysis of variance (Table 4) revealed that the predictability of the model is at 95% confidence interval. The ANOVA of this response verified that the model is highly significant as is observed from the value of $F_{\text{statistic}}=24.83$ (the ratio of regression mean square to the real error mean square), and a very low probability value ($P = 0.001$). The value of probability $P < 0.05$ reveals that the model is statistically significant [37].

In this study, A, B, AB, and C^2 were significant factors. C may be slightly significant ($P = 0.051$). The other model terms whose p greater than (0.05) are not significant factors. These results indicate that specific surface area is more related to current density and nickel ion concentration as individuals or a combination of them.

Table 4. ANOVA results for the quadratic equation for specific surface area of nickel powder

Source	DF	Seq SS	Contr. (%)	Adj SS	Adj MS	F-Value	P-Value
Model	9	0.674467	97.81	0.647420	0.074941	24.83	0.001
Linear	3	0.569308	82.56	0.569308	0.189769	62.87	0.000
A- Current Density(mAcm ⁻²)	1	0.449826	65.23	0.449826	0.449826	149.02	0.000
B-nickel sulfate concentration(gL ⁻¹)	1	0.099681	14.46	0.099681	0.099681	33.02	0.002
C-Temperature(°C)	1	0.019800	2.87	0.019800	0.019800	6.56	0.051
Square	3	0.054777	7.94	0.054777	0.018259	6.05	0.041
A ²	1	0.012737	1.85	0.016287	0.016287	5.40	0.068
B ²	1	0.000029	0.00	0.000108	0.000108	0.04	0.857
C ²	1	0.042010	6.09	0.042010	0.042010	13.92	0.014
2-Way Interaction	3	0.050382	7.31	0.050382	0.016794	5.56	0.047
AB	1	0.048400	7.02	0.048400	0.048400	16.03	0.010
AC	1	0.000650	0.09	0.000650	0.000650	0.22	0.662
BC	1	0.001332	0.19	0.001332	0.001332	0.44	0.536
Error	5	0.015093	2.19	0.015093	0.003019		
Lack-of-Fit	3	0.015074	2.19	0.015074	0.005025	538.37	0.002
Pure Error	2	0.000019	0.00	0.000019	0.000009		
Total	14	0.689560	100.00				
Model Summary	S		R ²	Adj-R ²		PRESS	
	0.0549416		97.81%	93.87%		0.24123	

In the present work, coefficient of determination (R^2) of 0.9781 and an Adj- R^2 of 0.9387 at a level of confidence of 95% were obtained for the quadratic equation model. Joglekar [38] proposed that a well model fit should produce value of R^2 higher than 0.8. This means that the response model estimated in this work can elucidate the relation between process variables and specific surface area of electrolytic nickel powder as well. The results of ANOVA show that current density has the major contribution at 65.23% (in linear term) followed by nickel sulfate concentration at 14.46% while temperature has the lower contribution at 2.87%. This is an indication that current density has the main effect on the surface area. Results of our previous work [39] related to the electrolytic zinc powder showed that zinc ion concentration has the main effect followed by current density while temperature has a little effect. This discrepancy may be resulted from the deference in electrode potentials where zinc has a more negative potential than nickel.

3.2. Effect of variables on the specific surface area of nickel powder

The combined effects of the three factors can be observed by using experimental design which is difficult to predict in conventional methods. The effects of factors on the specific surface area of nickel powder are shown in Figs. 3-5. These figures involve 3-D response surface plots of interactions between two factors on the specific surface area maintaining the third factor constant at zero level, and Contour

plots which are two-dimensional pictures of the response for selected factors. The contour plots are the projections of the response surfaces in the x–y plane that give a direct determination of the effects of variables on the response. An elliptical contour plot reveals that the interactions between them are significant while a circular contour plot reveals that no interactions could be existed [40].

The surface plot in Fig.3 reveals that the specific surface area of Ni powder strongly increases as the current density increases or decreasing of nickel sulfate concentration, the corresponding contour plot confirms that a maximum value of specific surface area lies in a smallest elliptic curve area in which the current density ranged between 450–500 mAcm⁻² and nickel sulfate concentration between 20–23 gL⁻¹. the contour plot shows an interaction between current density and sulfate concentration. In Fig. 4, a slight increase in the specific surface area of nickel powder was observed as nickel sulfate concentration and temperature decreased. The contour plot shows a semicircular curve area in which the surface area maximized. A maximum value could be obtained at a temperate range (35–45°C) and concentration range (20–23 gL⁻¹). No interaction between these variables was detected.

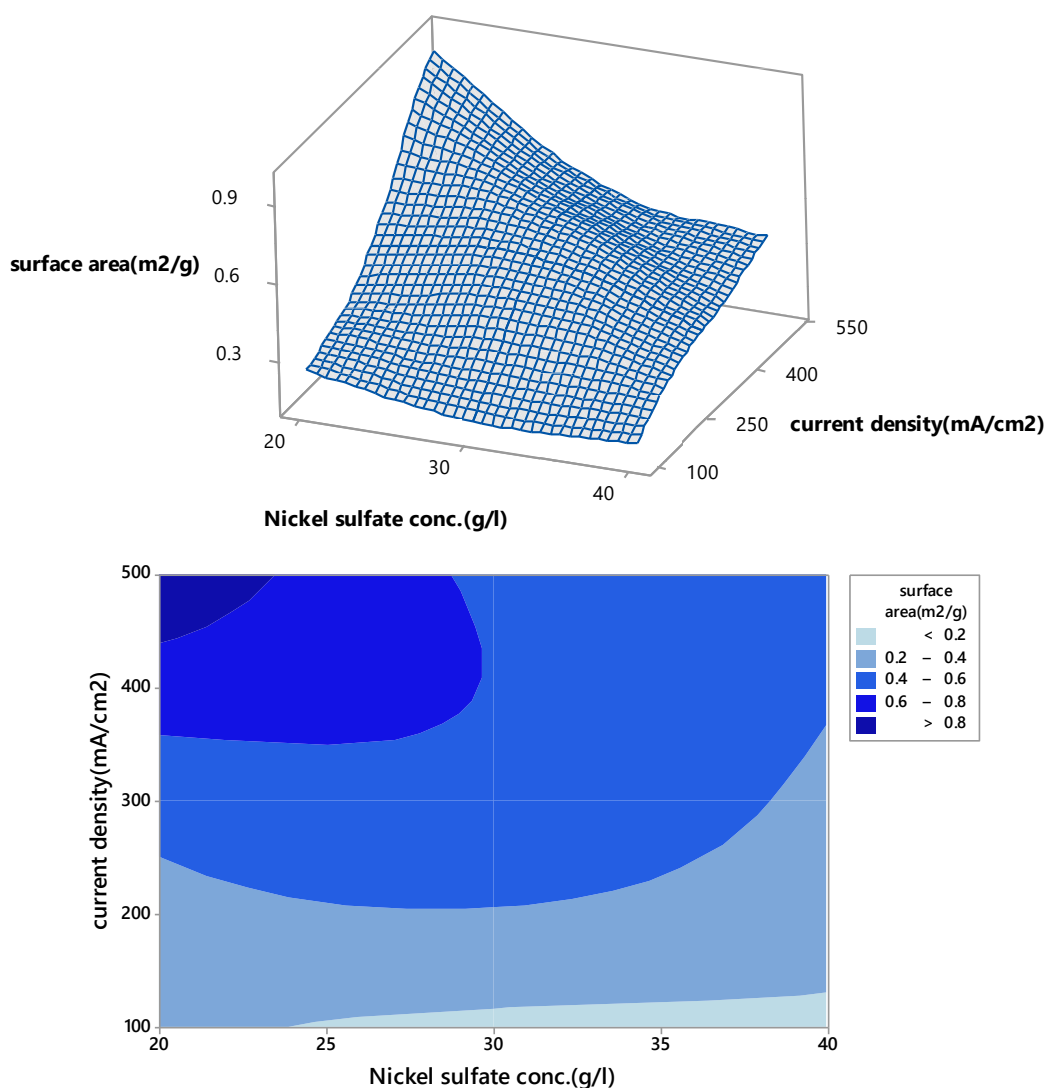


Figure 3. Response surface plot and contour plot of the specific surface area of nickel powder vs. current density and nickel sulfate concentration, temperature=45°C

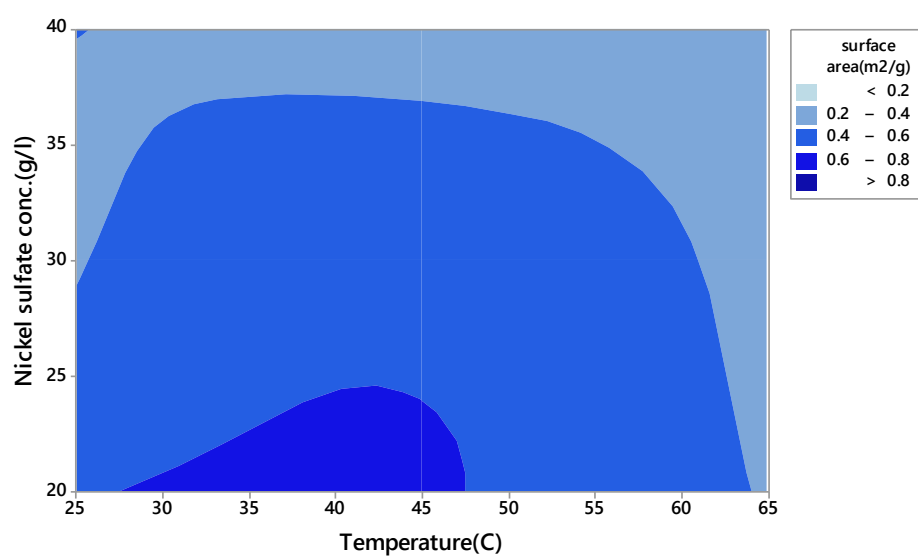
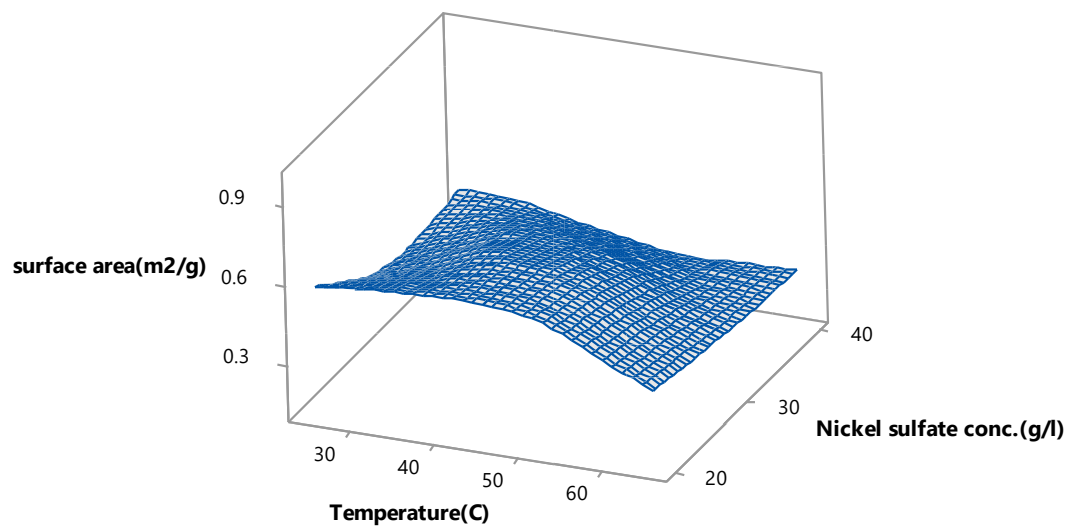
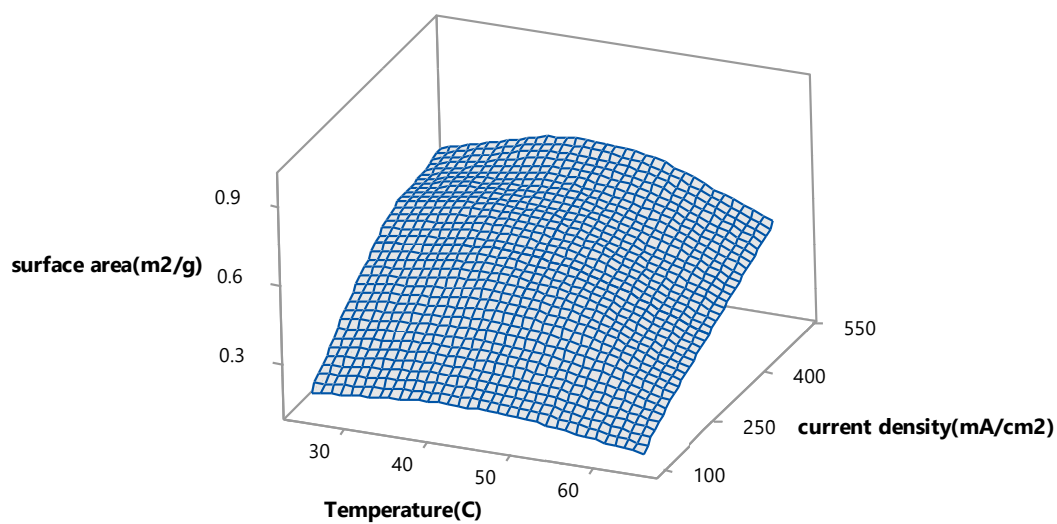


Figure 4. Response surface plot and contour plot of the specific surface area of nickel powder vs. nickel sulfate concentration and temperature, current density = 300 mA cm⁻²



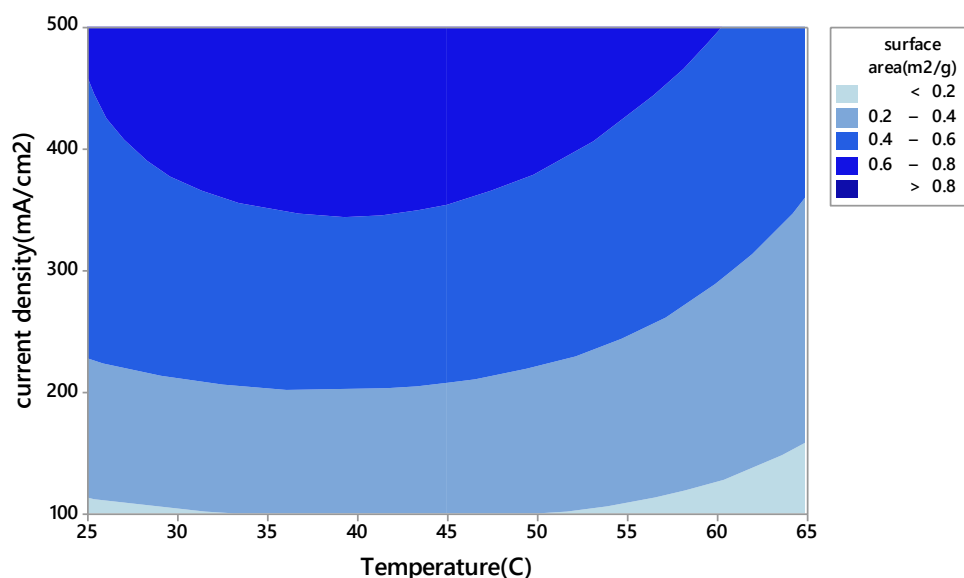


Figure 5. Response surface plot and contour plot of the specific surface area of nickel powder vs. current density and temperature, nickel sulfate concentration = 30 gL^{-1}

Fig.5 displays the surface plot of current density and temperature verses specific surface area. As can be seen, increasing the current density leads to strongly increasing in the surface area while a slight increase in the surface area of powder was found as the temperature decreased. Contour plot shows a circular curve region in which the surface area is maximized however no interaction between these variables was found.

All surface and contour plots confirm that current density has the major and strong effect on the specific surface area of nickel powder. This observation could be attributed to the enhancement of hydrogen evolution on the cathode due to the increase in the cathodic potential as the current density increases and this in turn gives more fine, porous, and nodular dendritic structure of the deposits [12]. On the other hand, present results show that the temperature has no significant effect which is in agreement with our previous work [39].

3.3. Conditions optimization and confirm tests

The numerical optimization of the software has been selected so as to discover the specific point that maximizes the desirability function. The desired goal was chosen by regulating the weight or importance that might change the goal characteristics. The goal ranges for the response of the model have five options: none, minimum, maximum, target and within range. The goal for the specific surface area of the powder is designated as 'maximum' with corresponding 'weight' 1.0. The lower limit value of the specific surface area is allocated at $0.124 \text{ m}^2 \text{ g}^{-1}$ while the upper limit value allocates at $0.98 \text{ m}^2 \text{ g}^{-1}$. The optimization procedure was performed under these settings and restrictions. The optimum values of the process variables in maximizing specific surface area are shown in Table 5 with desirability function of 0.95.

One of the main goals of this work is to confirm the result acquired for RSM-based optimized process factors. For their confirmation, duplicate confirmatory runs were achieved using the optimized factors. It was found that the average specific area is $1.05 \text{ m}^2\text{g}^{-1}$ which lies within 95% CI as shown in Table 6. These results confirm that Box-Behnken design could be efficiently employed to optimize the process operating factors in the electrolytic preparation of metal powders using the statistical design of experiments

Table 5. Optimum of process parameters for maximum specific surface area of nickel powder

Response		Goal	Lower	Target	Upper	Weight	Importance		
surface area(m ² g ⁻¹)		maximum	0.124	0.98	0.98	1	1		
Solution:			Parameters		Results				
C.D (mAcm ⁻²)	[NiSO ₄ .7H ₂ O] (gL ⁻¹)	T (°C)	Surface area (m ² g ⁻¹)	Fit	Composite Desirability	SE Fit	95% CI	95% PI	
500	20	37.5	0.9375		0.95	0.049	(0.8106; 1.0645)	(0.7476; 1.1274)	

Table 6. Confirmative value of the optimum surface area

A (mAcm^{-2})	B (gL^{-1})	C ($^{\circ}\text{C}$)	Weight (g)	E (Volt)	surface area (m^2g^{-1})	CE (%)	EC (kWhkg^{-1})
500	20	38	1.848	7.86	1.05	30	24.0

3.4. Characterization of nickel powder

Fig.6 shows a typical XRD pattern of Nickel powder prepared at the optimum conditions. From the Figure, three characteristic peaks for Nickel [$2\theta = 44.5^{\circ}$, 51.86° , 76.44°] corresponding to Miller indices (111), (200), (220) were observed. This confirms that the resultant powder was pure Nickel. The produced nickel powder proved to be very pure with no hydroxide or oxide contamination. In addition, the data obtained confirm that nickel is deposited in a polycrystalline form with face-centered cubic (FCC) structure. Based on the AFM results shown in Fig. 7, the prepared nickel powder has an average particle size of 680.65 nm. The surface morphology and shape of the produced nickel powder is displayed in Fig.8. It was clear that the prepared nickel powder has particles having the shape of classical dendrite structure.

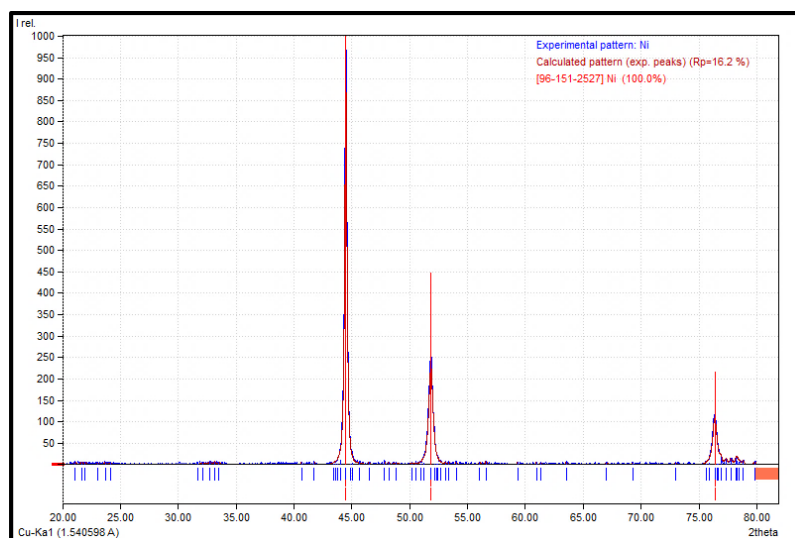


Figure 6. XRD diffraction pattern of the electrolytic nickel powder

Based on the results of BTE, XRD, AFM, it was observed that the prepared powder has excellent properties in comparison with the industrial nickel powder (Type 255-carbonyl process) that has a purity of 99.7% , an average particle size in the range (2.2 - 2.8 μm), and a specific surface area of $0.68 \text{ m}^2\text{g}^{-1}$ [41].

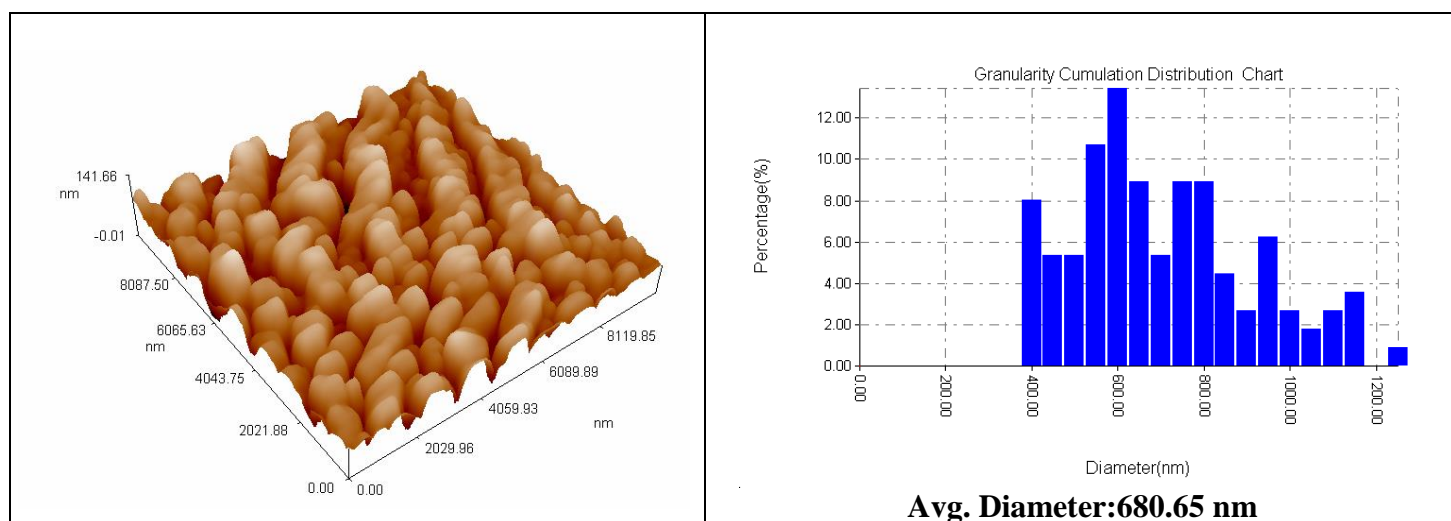


Figure 7. AFM results of nickel powder.

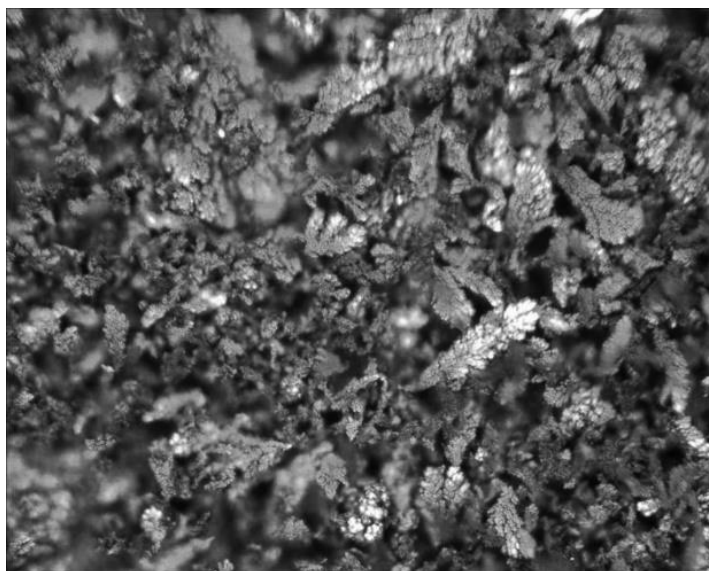


Figure 8. Optical micrograph of the optimum nickel powder. Magnification, 100X

4. CONCLUSIONS

From the results presented in this work it could be concluded that current density has the important role on the specific surface area of nickel powder while a sensitive role of metal ion concentration was observed with no effect of temperature. The Box–Behnken design was successfully used to create a mathematical model for predicting the specific surface area of nickel powder. The value of $R^2 > 0.9781$ for the obtained quadratic model shows that there is high correlation between experimental results and predicted values by the model. Numerical Optimization using RSM gave optimum operating conditions as current density of 500 mAcm^{-2} , nickel sulfate concentration of 20 gL^{-1} , and temperature of 38°C yielding a specific surface area of powder of $1.05 \text{ m}^2\text{g}^{-1}$. Under these optimum conditions, a current efficiency of 30% was observed, which is higher than the previous works. Interestingly, 3D-response surface plots combined with contour plots can be the suitable way for observing parameter interactions where a clear interaction between current density and nickel sulfate concentration was observed.

It should be emphasized that the first results on using of response surface methodology for studying the effect of interaction among electrolysis parameters on the specific surface area of metal powder are presented in this work and this methodology may be successfully used to study the importance of the individual, cumulative, and interactive effects of process variables in preparation of other metallic powders.

ACKNOWLEDGMENTS

The authors wish to acknowledge the gracious technical assistance from the staff of the Chemical Engineering Department, College of Engineering-University of Al-Qadissiyah, specially the engineers: H. A. Shamghi, Z. N. Abbas, and Z. N. Abdul-Hadi.

References

1. A. Calusaru, *Electrodeposition of Metal Powders*, Elsevier, (1979) Amsterdam, The Netherlands. p. 299, 303, 377.
2. I. Šafařík and M. Šafaříková, *Monatshefte. Fuer. Chemie*. 133 (2002) 737.
3. A. I. Gusev, *Phys. Usp.*, 41(1998) 49.
4. O. D. Neikov, I. B. Murashova, N. A. Yefimov and S. Naboychenko, *Handbook of Non-Ferrous Metal Powders: Technologies and Applications*, Elsevier Science, (2009) Amsterdam, The Netherlands.
5. J. M. Capus, *Metal Powders: A Global Survey of Production, Applications and Markets 2001-2010*, Fourth edition, Elsevier, (2005) Amsterdam, The Netherlands. p.90.
6. I. B. Murashova, *Electrochemical Methods of Metal Powder Production* in: O. D. Neikov, I. B. Murashova, N. A. Yefimov, S. Naboychenko, *Handbook of Non-Ferrous Metal Powders: Technologies and Applications*, Elsevier, (2009) Amsterdam, The Netherlands. p.181-211.
7. G. Wranglen, *Acta Polytech. Electr. Eng. Ser. 2*(1950)69.
8. R.M. Khalil, *J. Appl. Electrochem.*, 18 (1988) 292.
9. S.G. Viswanath and M. M. Jachak, *Metall. Mater. Eng.*, 19 (2013) 233.
10. C. L. Mantell, *Production of nickel powder* (1941) USA Patent No. 2233103.
11. A. M. Abd El-Halim, A. O. Baghlaf and R.M. Khalil, *Powder Technol.*, 43(1985)103.
12. A.M. Abd El-Halim and R.M. Khalil, *Surface Technology*, 26 (1985) 343.
13. D.K. Borikar, S.S. Umare and S.G. Viswanath, *Metalurgija* 45 (2006) 3.
14. O. I. Kuntiyi, *Russ. J. Non-ferrous Metals*, 48(2007)17.
15. S.G. Viswanath and G. Sajimol, *Metall. Mater. Eng.*, 18 (2012)129.
16. V. D. Jović, V. Maksimović, M. G. Pavlović and K. I. Popov, *J. Solid State Electrochem.*, 10 (2006) 373.
17. K. Appelt, Z. Dominiczak, A. Nowacki and M. Paszkiewicz, *Electrochem. Acta*, 10 (1965) 617.
18. C. L. Mantell, *J. Electrochem. Soc.*, 106 (1959)70.
19. B. B. Bagalkote and J. G. Kane, *ind. J. Appl.Chem.* 24 (1961) 29.
20. S.V. Kupin and B. S. Yurev, *Poroshkovaya Metall* (Translated) 145(1973) 20.
21. A.S. Kurlov, A.I. Gusev and A.A. Rempel, *Rev.Adv.Mater. Sci.*, 32 (2012) 52.
22. A.V. Pomosov and I.B. Murashova, *Powder Metall. Met. Ceram.*, 5 (1966)433.
23. M. Lucaci, S. Gavrilu, M. Lungu, I. Vida Simiti and I. Roman, *J. Optoelectron. Adv. M.*, 6 (2004) 947.
24. M.A. Bezerra, R.E. Santelli, E.P. Oliveira, L.S. Villar and L.A. Escaleira, *Talanta*, 76 (2008)965.
25. P.D. Haaland, *Statistical Problem Solving*, In: P.D. Haaland, *Experimental Design in Biotechnology*, Marcel Dekker, (1989) New York. p.1-18.
26. M. Tir and N. Moulai-Mostefa, *Desalin. Water Treat.*, 7 (2009) 214.
27. G.E.P. Box and D.W. Behnken, *Technometrics*, 2(1960)455.
28. S.L.C. Ferreira, R.E. Bruns, H.S. Ferreira, G.D. Matos, J.M. David, G.C. Brandao, E.G.P. Dasilva, L.A. Portugal, P.S. Dos Reis, A.S. Souza and W.N.L. Dos Santos, *Anal. Chim. Acta*, 597(2007)179.
29. M.Y. Can, Y. Kaya and O.F. Algur, *Bioresour. Technol.*, 97(2006)1761.
30. M. Meilgaard, G.V. Civile and B.T. Carr, *Advanced Statistical Methods, Sensory Evaluation Techniques*, 2nd ed., CRC Press, (1991) Boca Raton, FL. p. 275.
31. B. Sharifi, M. Mojtahedi, M. Goodarzi and J. Vahdate Khaki, *Hydrometallurgy*, 99 (2009)72.
32. G. Kreysa, *J. Appl. Electrochem.*, 15(1985)175.
33. A. I. Khuri and S. Mukhopadhyay, *Response surface methodology*, *WIREs Comp Stat* 2(2010)128-149.
34. E. Hamed and A. Sakr, *J. Controlled Release*, 73 (2001) 329.
35. P. Qiu, M. Cui, K. Kang, B. Park, Y. Son, E. Khim, M. Jang and J. Khim, *cent. eur. j. chem.*, 12 (2014)164.

36. R. Arunachalam and G. Annadurai, *J. Environ. Sci. Technol.*, 4 (2011) 65.
37. M.S. Phadke, *Quality Engineering Using Robust Design*, Prentice Hall, (1989) New Jersey, USA.
38. A.M. Joglekar, and A.T. May, *Cereal Food World*, 32(1987)857.
39. A. H. Abbar, S. A. Rushdi and H. M. Al-Tameemi, *Int. J. Electrochem. Sci.*, 12(2017)7075.
40. J. Aravind, C. Lenin, C. Nancyflavia, P. Rashika and S. Saravanan, *Int. J. Environ. Sci. Technol.*, 12 (2015)105.
41. V. A. Tracey, *Powder Metall.*, 9(1966)54.

© 2019 The Authors. Published by ESG (www.electrochemsci.org). This article is an open access article distributed under the terms and conditions of the Creative Commons Attribution license (<http://creativecommons.org/licenses/by/4.0/>).